

Article

Bismercaptoethanediazacyclooctane as a NS Chelating Agent and Cys–X–Cys Mimic for Fe(NO) and Fe(NO)

Chao-Yi Chiang, Matthew L. Miller, Joseph H. Reibenspies, and Marcetta Y. Darensbourg

J. Am. Chem. Soc., **2004**, 126 (35), 10867-10874 • DOI: 10.1021/ja049627y • Publication Date (Web): 11 August 2004

Downloaded from <http://pubs.acs.org> on April 1, 2009

More About This Article

Additional resources and features associated with this article are available within the HTML version:

- Supporting Information
- Links to the 5 articles that cite this article, as of the time of this article download
- Access to high resolution figures
- Links to articles and content related to this article
- Copyright permission to reproduce figures and/or text from this article

[View the Full Text HTML](#)



Bismercaptoethanediazacyclooctane as a N₂S₂ Chelating Agent and Cys–X–Cys Mimic for Fe(NO) and Fe(NO)₂

Chao-Yi Chiang, Matthew L. Miller, Joseph H. Reibenspies, and Marcetta Y. Darensbourg*

Contribution from the Department of Chemistry, Texas A&M University, College Station, Texas 77843

Received January 21, 2004; E-mail: marcetta@mail.chem.tamu.edu

Abstract: The N-protonated bismercaptoethanediazacyclooctane serves as a bidentate dithiolate ligand to oxidized Fe(NO)₂ of Enemark–Feltam notation, E–F {Fe(NO)₂},⁹ mimicking Cys–X–Cys binding of Fe(NO)₂ to proteins or thio-biomolecules. The neutral compound is characterized by the well-known *g* = 2.03 EPR signal which is a hallmark of dinitrosyl iron complexes, DNIC's. The Fe(NO)₂ unit can be removed from the chelate by excess PhS[–], producing (PhS)₂Fe(NO)₂[–]. Transfer of NO from Fe(H⁺bme-daco)(NO)₂ ($\nu(\text{NO}) = 1740, 1696 \text{ cm}^{-1}$) to Fe^{II} of [(bme-daco)Fe]₂ yields the five-coordinate, square-pyramidal N₂S₂-Fe(NO) ($\nu(\text{NO}) = 1649 \text{ cm}^{-1}$), where NO is in the apical position. Its isotropic EPR signal at *g* = 2.05 is consistent with E–F {Fe(NO)}⁷ formulation. In excess NO, Roussin's red ester-type molecules are formed as dinuclear or tetranuclear species, $\{(\mu\text{-SRS})[\text{Fe}_2(\text{NO})_4]\}_n$ (*n* = 1, 2). These well-characterized molecules furnish reference points for positions and patterns in $\nu(\text{NO})$ vibrational spectroscopy expected to be useful for in vivo studies of NO degradation of iron–sulfur clusters in ferredoxins.

Introduction

The interactions of NO with sulfur of natural thiols, forming nitrosothiols (RSNO'S),^{1–3} and with heme iron in hemoglobin or myoglobin, forming nitrosylated or RS-nitrosylated heme,^{3–5} have been intensely studied by chemists and biochemists. Also well known in bioinorganic chemistry is the iron–nitrosyl found in the NO-deactivated form of iron–nitrile hydratase.^{6,7} The unusual binding site is composed of deprotonated carboxamido nitrogens in a cysteine–serine–cysteine sequence within the protein, resulting in a planar array of N₂S₂ donor sites. As shown in structure **A**, two of the cysteine sulfurs in the N₂S₂ moiety are further modified as S-oxygenates. Photolabilization of the NO is required for enzyme activity.

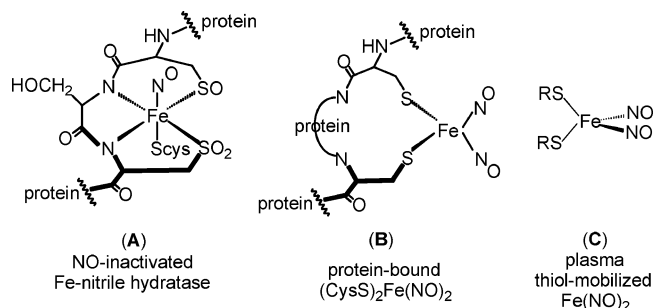
Yet another “natural” Fe–NO complex, a tetrahedral, S-bound iron dinitrosyl, has been known for decades.^{8,9} Interest in sulfur-bound dinitrosyl iron complexes (DNIC's) derives from their fundamental properties and the possibility of physiologically significant chemistry.^{9,10} The latter includes degradation

of iron–sulfur clusters to produce (protein–Cys–S)₂Fe(NO)₂[–], **B**, which was discovered in studies of 2Fe₂S and 4Fe₄S ferredoxins, in the presence of excess NO.^{11–14} A repair process established by Ding et al. requires L-cysteine and cysteine desulfurase to remove NO and provide sulfur for the regeneration of the iron–sulfur clusters.^{12–14} An undetermined issue is whether, or the conditions under which, the protein-bound DNIC may be mobilized by reaction with plasma thiols such as glutathione or free cysteine, thereby becoming potential NO carriers, **C**.¹⁵ In this connection, DNIC's have been suggested to serve as labile NO sources similarly to RSNO's, showing the same biological activities such as vasodilation.^{16,17} As yet another possible physiological action, the intracellular formation of DNIC's has been suggested to reduce NO cytotoxicity.¹⁸ The scope of these processes has inspired us to examine the inorganic/organometallic precedents of import to DNIC's.

The inorganic literature finds precedents for small molecule DNIC's in two oxidation levels of the Fe(NO)₂ unit. A diamagnetic, reduced form is stabilized by soft donor ligands such as CO and PR₃ in neutral L₂Fe(NO)₂ complexes;^{19,20} a paramagnetic, oxidized form, [X₂Fe(NO)₂][–], is found with

- (1) Williams, D. L. H. *Acc. Chem. Res.* **1999**, *32*, 869–875.
- (2) Wang, P. G.; Xiao, M.; Tang, X.; Wu, X.; Wen, Z.; Cai, T.; Janczuk, A. *J. Chem. Rev.* **2002**, *102*, 1091–1134.
- (3) Richardson, G.; Benjamin, N. *Clin. Sci.* **2002**, *102*, 99–105.
- (4) (a) Möller, J. K. S.; Skibsted, L. H. *Chem. Rev.* **2002**, *102*, 1167–1178. (b) Wyllie, G. R. A.; Scheidt, W. R. *Chem. Rev.* **2002**, *102*, 1067–1090.
- (5) Müller, B.; Kleschyov, A. L.; Alencar, J. L.; Vanin, A.; Stoclet, J.-C. *Ann. N.Y. Acad. Sci.* **2002**, *962*, 131–139 and references therein.
- (6) Mascharak, P. K. *Coord. Chem. Rev.* **2002**, *225*, 201–214.
- (7) Nagashima, S.; Nakasako, M.; Dohmae, N.; Tsujimura, M.; Takio, K.; Odaka, M.; Yohda, M.; Kamiya, N.; Endo, I. *Nat. Struct. Biol.* **1998**, *5*, 347–351.
- (8) Vithayathil, A. J.; Ternberg, J. L.; Commoner, B. *Nature* **1965**, *207*, 1246–1249.
- (9) Woolum, J. C.; Commoner, B. *Biochim. Biophys. Acta* **1970**, *201*, 131–140.
- (10) Kleschyov, A. L.; Hubert, G.; Munzel, T.; Stoclet, C.; Bucher, B. *BMC Pharmacol.* **2002**, *2*, 3.

- (11) Foster, M. W.; Cowan, J. A. *J. Am. Chem. Soc.* **1999**, *121*, 4093–4100.
- (12) Rogers, P. A.; Ding, H. *J. Biol. Chem.* **2001**, *276*, 30980–30986.
- (13) Yang, W.; Rogers, P. A.; Ding, H. *J. Biol. Chem.* **2002**, *277*, 12868–12873.
- (14) Rogers, P. A.; Eide, L.; Klungland, A.; Ding, H. *DNA Repair* **2003**, *2*, 809–817.
- (15) Lobysheva, I. I.; Serezhnikov, V. A.; Stukan, R. A.; Bowman, M. K.; Vanin, A. F. *Biochemistry (Moscow)* **1997**, *62*, 801–808.
- (16) Vedernikov, Y. P.; Mordvintsev, P. I.; Malenkova, I. V.; Vanin, A. F.; *Eur. J. Pharmacol.* **1992**, *211*, 313–317.
- (17) Vanin, A. F.; Stukan, R. A.; Manukhina, E. B. *Biochim. Biophys. Acta* **1996**, *1295*, 5–12.
- (18) Kim, Y. M.; Chung, H. T.; Simmons, R. L.; Billiar, T. R. *J. Biol. Chem.* **2000**, *275*, 10954–10961.



halide, pseudo-halide, and thiolate ligands.^{21,22} The latter is characterized by an isotropic EPR signal of $g = 2.03$ – 2.04 ; in fact, it was this spectroscopic feature that first linked the inorganic models to the biological DNIC's.²³ The Fe(NO)₂ units in these as well as in the (RS)₂Fe(NO)₂[−] complexes are computed to carry a +1 charge and are designated according to the Enemark–Feltham (E–F) notation (a summation of Fe^d d-electrons and the number of NO ligands) as {Fe(NO)₂}¹.²⁴ The reduced, diamagnetic form, denoted as E–F {Fe(NO)₂}⁰, has a charge of 0 in the neutral L₂Fe(NO)₂ complexes where L is a soft donor. Borderline hard/soft donors such as nitrogen in imidazoles produce the Fe(NO)₂ unit in forms that appear to easily convert between oxidized and reduced redox levels.²⁵ A pertinent example comes from DNIC's derived from histidine mimics such as that of Li and co-workers.²⁵

Because of its sensitivity at low concentrations, EPR spectroscopy is the most frequently used diagnostic for biological DNIC species. However, a review of the available data shows little differences in the g values for potential model species of quite different compositions, including those that, based on bulk composition and structures, should be diamagnetic. The latter discrepancy results from solution studies where small amounts of the complex may be solvated leading to oxidation and EPR activity.^{26,27} A further complicating feature of DNIC detection and characterization is that further oxidation in solution forms the stable and EPR silent Roussin's red "esters" of formulation (μ-SR)₂Fe₂(NO)₄. Hence, it is important to develop an auxiliary technique for DNIC identification and study; $\nu(\text{NO})$ vibrational spectroscopy is an obvious choice.

We have explored the use of {Fe(NO)₂} as a redox active reporter unit in heterometallic complexes based on (RS)₂Fe(NO)₂[−].²⁸ The oxidation level of the {Fe(NO)₂} unit in Ni(μ-

SR)₂Fe(NO)₂[−] is dependent on the oxidation state of Ni, thus placing the Ni(0) derivative, [(ON)Ni⁰(μ-S(CH₂)₂S(CH₂)₂S)Fe(NO)₂], in the same class as the paramagnetic, $g = 2.03$, oxidized version of (RS)₂Fe(NO)₂[−]. In contrast, the Ni(II) derivatives using the N₂S₂ dithiolate ligands such as (bismercaptoethanediazacyclooctane)nickel(II), (bme-daco)Ni(II), as the metallthiolate ligand to {Fe(NO)₂} generated the neutral, reduced L₂Fe(NO)₂ complexes, similarly to diphosphine derivatives, (Ph₂PCH₂CH₂PPh₂)Fe(NO)₂.²⁸

The following report is of chemistry developing from our attempts to generate the nickel-free versions of [(−S(CH₂)₂S(CH₂)₂S)[−]Fe(NO)₂][−] and (bme-daco)Fe(NO)₂[−] which have led to unique structural forms. For the former, a tetranuclear dimer of dimers defines a Roussin's red "ester" with a symmetrical orientation of μ-SR units. The latter demonstrates a novel configuration of the structurally reinforced diaza ligand that can accommodate a tetrahedral (RS)₂Fe(NO)₂[−] structure, an analogue of biological (Cys–X–Cys)₂Fe(NO)₂[−]. Transfer of one NO to an NO acceptor shifts the remaining FeNO unit into the N₂S₂ core. The preparation and characterization of these structural types of nitrosyl iron complexes, including explorations of an RS[−] ligand exchange process and NO transfer from (H⁺bme-daco)[Fe(NO)₂], are described below. Notably this well-characterized series provides vibrational spectroscopic reference points and uses vibrational spectroscopy as a monitor for reaction pathways of iron nitrosyls in biologically significant sulfur-rich coordination.

Experimental Section

Materials and Techniques. Solvents were of reagent grade and purified as follows: Dichloromethane was distilled over P₂O₅ under N₂. Acetonitrile was distilled once from CaH₂, once from P₂O₅, and freshly distilled from CaH₂ immediately before use. Diethyl ether, toluene, THF, and hexane were distilled from sodium/benzophenone under N₂. Syntheses of PPN[FeI₂(NO)₂],²¹ Na₂(SCH₂CH₂SCH₂CH₂S),²⁹ N,N'-bis(2-mercaptoethyl)-1,5-diazacyclooctane (H₂bme-daco),³⁰ and its iron complex, [(bme-daco)Fe]₂,³¹ were according to published procedures. NO gas (98.5%) and 2-mercaptoethyl sulfide (90%) were purchased from Aldrich Chemical Co. and were used as received. Syntheses and manipulations were performed using standard Schlenk-line and syringe/rubber septa techniques under N₂ or in an argon atmosphere glovebox. Filtrations of solutions used airless-ware glass frits typically with 1–2 cm pads of Celite.

Infrared spectra were recorded on a Mattson 6022 spectrometer in a CaF₂ cell of 0.1 mm path length. UV/vis spectra were recorded on a Hewlett-Packard HP8452A diode array spectrophotometer. Elemental analyses were performed by Canadian Microanalytical Systems in Delta, British Columbia, Canada. Electro-spray ionization mass spectrometry data were obtained at the Laboratory for Biological Mass Spectrometry, Texas A&M University, College Station, Texas, using a MDS Series Qstar Pulsar with a spray voltage of 5 keV. The EPR spectrum was recorded on a Bruker X-band EPR spectrometer (model ESP 300E) with an Oxford Liquid Helium/Nitrogen cryostat at 77 K in CH₂Cl₂, 1 mW power, and 0.1 mT modulated amplitude.

Preparations. (H⁺bme-daco)Fe(NO)₂, Complex 1. In a typical synthesis, a 0.268 g (1.15 mmol) portion of H₂bme-daco dissolved in

- (19) (a) Brockway, L. O.; Anderson, J. S. *Trans. Faraday Soc.* **1937**, *33*, 1233–1239. (b) Hedberg, L.; Hedberg, K.; Sattija, S. K.; Swanson, B. I. *Inorg. Chem.* **1985**, *24*, 2766–2771.
- (20) Albano, V. G.; Araneo, A.; Bellon, P. L.; Ciani, G.; Manassero, M. J. *Organomet. Chem.* **1974**, *67*, 413–422.
- (21) Connelly, N. G.; Gardner, C. J. *Chem. Soc., Dalton Trans.* **1976**, 1525–1527.
- (22) Strasdeit, H.; Krebs, B.; Henkel, G. Z. *Naturforsch.* **1986**, *41b*, 1357–1362.
- (23) (a) Butler, A. R.; Glidewell, C.; Johnson, I. L.; Walton, J. C. *Polyhedron* **1987**, *6*, 2085–2090. (b) McDonald, C. C.; Phillips, W. D.; Mower, H. F. *J. Am. Chem. Soc.* **1965**, *87*, 3319–3326. (c) Basosi, R.; Gaggelli, E.; Tiezzi, E.; Valensin, G. *J. Chem. Soc., Perkin Trans. 2* **1975**, 423–428. (d) Jezowska-Trezebiatowska, B.; Jezierski, A. *J. Mol. Struct.* **1973**, *19*, 635–640. (e) Bryar, T. R.; Eaton, D. R. *Can. J. Chem.* **1992**, *70*, 1917–1926.
- (24) Enemark, J. H.; Feltham, R. D. *Coord. Chem. Rev.* **1974**, 340–404.
- (25) (a) Reginato, N.; McCrory, C. T. C.; Pervitsky, D.; Li, L. *J. Am. Chem. Soc.* **1999**, *121*, 10217–10218. (b) Li, L. *Comments Inorg. Chem.* **2000**, *23*, 335–353.
- (26) Burlamacchi, L.; Martini, G.; Tiezzi, E. *Inorg. Chem.* **1969**, *8*, 2021–2025.
- (27) Li, L.; Morton, J. R.; Preston, K. F. *Magn. Reson. Chem.* **1995**, *33*, S14–S19.
- (28) Liaw, W.-F.; Chiang, C.-Y.; Lee, G.-H.; Peng, S.-M.; Lai, C.-H.; Darenbourg, M. Y. *Inorg. Chem.* **2000**, *39*, 480–484.

- (29) Yogi, S.; Hokama, K.; Tsuge, O. *Bull. Chem. Soc. Jpn.* **1987**, *60*, 335–342.
- (30) Mills, D. K.; Font, I.; Farmer, P. J.; Tuntulani, T.; Buonomo, R. M.; Goodman, D. C.; Musie, G.; Grapperhaus, C. A.; Maguire, M. J.; Lai, C.-H.; Hatley, M. L.; Smees, J. J.; Bellefeuille, J. A.; Darenbourg, M. Y. *Inorg. Synth.* **1998**, *32*, 89–98.
- (31) Mills, D. K.; Hsiao, Y. M.; Farmer, P. J.; Atnip, E. V.; Reibenspies, J. H.; Darenbourg, Y. D. *J. Am. Chem. Soc.* **1991**, *113*, 1421–1423.

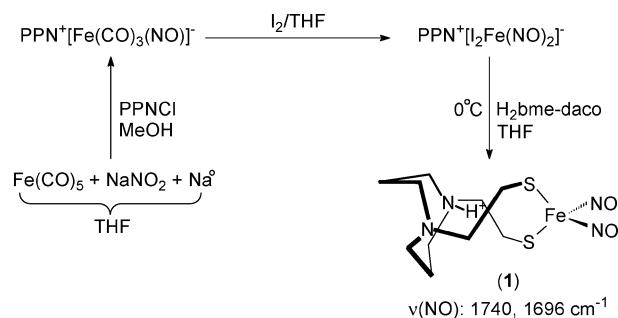
10 mL of THF was transferred into a 50 mL Schlenk flask containing a stir bar and 0.365 g (0.40 mmol) of $\text{PPN}^+[\text{Fe}(\text{CO})_3(\text{NO})]^-$, which was immersed in a 0 °C bath. The reaction mixture was maintained at 0 °C with stirring for 2 h. The solvent was removed under vacuum, and the resulting brown green oil was redissolved in MeOH. Under air-free conditions, degassed water was added and the solid which precipitated was collected on a filter frit. The solid was redissolved in THF, and trace H_2O was removed by adding MgSO_4 . The solution was decanted from the drying agent, and the solvent was removed under vacuum. The resulting solid was washed with hexane before being redissolved in THF and filtered through Celite to remove PPN^+I^- . After removal of the solvent, crude solid (0.062 g, 44%) was collected. Brown-red crystals suitable for X-ray diffraction analysis were obtained by diffusion of pentane vapor into a THF solution of compound at 5 °C. Infrared spectrum (ν_{NO}): 1695(s), 1739(m) cm^{-1} (THF). The synthesis worked equally well with $\text{Et}_4\text{N}^+[\text{Fe}(\text{NO})_2]^-$ as starting material from which purer bulk samples were obtained, affording acceptable elemental analyses. Mass spectrum: $m/z = 350.05$ (complex **1** + H^+); 334.04 (complex **1** - (N + H)); 320 (complex **1** - NO). Also present $m/z = 465$ (complex **3** + H^+); 434 (complex $3\text{H}^+ - \text{NO}$); 404 (complex $3\text{H}^+ - 2\text{NO}$). Anal. Calcd for $\text{C}_{10}\text{H}_{21}\text{O}_2\text{N}_4\text{FeS}_2$: C, 34.39; H, 6.06; N, 16.04. Found: C, 34.10; H, 5.87; N, 15.14.

(bme-daco)Fe(NO), Complex 2. A 1.34 g (2.34 mol) portion of $[(\text{bme-daco})\text{Fe}]_2$ was dissolved in 70 mL of MeOH in a 100 mL Schlenk flask at 60 °C under argon. Under NO gas (1 atm), the solution color changed from purple-brown to green within 30 min. The solvent was removed under vacuum. The solid was redissolved in 50 mL of CH_2Cl_2 and filtered through Celite. The green filtrate was concentrated to 5 mL under vacuum, and addition of 30 mL of pentane resulted in precipitation of a green solid; yield 1.27 g, 86%. Green crystals of X-ray diffraction quality were obtained by diffusion of pentane vapor into a CH_2Cl_2 solution of complex **2** maintained at 5 °C. IR (ν_{NO}): 1649(s) cm^{-1} (CH_2Cl_2). Anal. Calcd for $\text{C}_{10}\text{H}_{20}\text{ON}_3\text{FeS}_2$: C, 37.74; H, 6.33; N, 13.20. Found: C, 37.27; H, 6.26; N, 12.87.

$\text{PPN}^+[(\text{S}_3')\text{Fe}(\text{NO})_2]^-$, Complex 4, and $\text{Fe}_4(\text{S}_3')_2(\text{NO})_8$ ($\text{S}_3' = \text{S}(\text{CH}_2)_2\text{S} - (\text{CH}_2)_2\text{S}$), Complex 5. The reaction of $\text{PPN}^+[\text{Fe}(\text{NO})_2]^-$ (0.363 g, 0.40 mmol) with $\text{Na}_2\text{S}_3'$, $\text{Na}_2(\text{SCH}_2\text{CH}_2\text{SCH}_2\text{CH}_2\text{S})$, (0.156 g, 0.80 mmol) in a 1:1 mixture of MeOH/THF resulted in a green solution with $\nu(\text{NO}) = 1694, 1739 \text{ cm}^{-1}$. All attempts to isolate and crystallize the presumed $\text{PPN}^+[(\text{S}_3')\text{Fe}(\text{NO})_2]^-$ salt resulted in conversion to a red-brown product with $\nu(\text{NO}) = 1751, 1777 \text{ cm}^{-1}$, THF solvent. In solution, even at -20 °C, the green $\text{PPN}^+[(\text{S}_3')\text{Fe}(\text{NO})_2]^-$, **4**, slowly changed to the red complex **5**. This product was determined by X-ray crystallography to be the tetranuclear $\text{Fe}_4(\text{S}_3')_2(\text{NO})_8$. As a solid, it is both thermally and air stable (for short periods); however, solutions should be kept under Ar or N_2 . It is soluble in THF and CH_2Cl_2 . Anal. Calcd for $\text{C}_8\text{H}_{16}\text{O}_8\text{N}_8\text{Fe}_4\text{S}_6 \cdot \text{CH}_3\text{OH}$: C, 13.51; H, 2.52; N, 14.01. Found: C, 14.0; H, 2.31; N, 13.8.

X-ray Structure Determinations. X-ray data were obtained on an Apex CCD diffractometer and covered a hemisphere of space upon combining three sets of exposures. The space groups were determined on the basis of systematic absences and intensity statistics. The structures were solved by direct methods. Anisotropic displacement parameters were determined for all non-hydrogen atoms. Hydrogen atoms were added at idealized positions and refined with fixed isotropic displacement parameters equal to 1.2 (1.5 for methyl protons) times the isotropic displacement parameters of the atoms to which they were attached. Atoms which proved to be nonpositive definite were corrected by including the command ISOR with the "s" parameter set at 0.05 in the instruction file. Programs used for data collection and cell refinement, SMART;³² data reduction, SAINT-Plus;³³ structure solution, SHELXS-86 (Sheldrick);³⁴ structure refinement, SHELXL-97 (Sheld-

Scheme 1



rick),³⁵ and molecular graphics and preparation of material for publication, SHELXTL-Plus, version 5.1 or later (Bruker).³⁶

Results and Discussion

Syntheses and Molecular Structures. Among several available routes for the synthesis of $(\text{RS})_2\text{Fe}(\text{NO})_2^-$ complexes, the method presented in Scheme 1 was selected for the N_2S_2 bme-daco derivatives. Following the procedure of Connelly and Gardner, reductive nitrosylation of $\text{Fe}(\text{CO})_5$ followed by oxidative addition of I_2 yields the $[\text{I}_2\text{Fe}(\text{NO})_2]^-$ anion, isolated as its PPN^+ salt.²¹ Reaction with excess of the dithiol, $\text{H}_2\text{bme-daco}$, in THF solution at 0 °C results in iodide displacement by the dithiolate and precipitation of PPN^+I^- . For mass balance, a mole of HI should be released. The brown-green complex **1** is obtained as a solid following removal of THF, redissolving in MeOH, precipitation on addition of H_2O , and recrystallization (THF/hexane or THF/pentane). The solid may be stored indefinitely in an Ar-filled glovebox freezer held at -35 °C. Long-term exposure (hours) of solutions of **1** to air, water, or heat leads to slow decomposition with formation of (bme-daco)- $\text{Fe}(\text{NO})$, complex **2**, or the Roussin's red ester complex, $[(\text{bme-daco})[\text{Fe}(\text{NO})_2]_2]_n$, $n = 1$ or 2 .

Optimal conditions for production of complex **1** in near quantitative yields as determined by solution $\nu(\text{NO})$ IR spectroscopy via Scheme 1 employ a ratio of $\text{H}_2\text{bme-daco}$ to $\text{PPN}^+[\text{I}_2\text{Fe}(\text{NO})_2]^-$ of ca. 3:1 in THF. Other solvents, CH_3CN , CH_2Cl_2 , and MeOH, may be used; however, at lower L:Fe ratios, a minor product is observed with $\nu(\text{NO}) = 1649 \text{ cm}^{-1}$. A direct route to this green product, (bme-daco)Fe(NO), complex **2**, is outlined in Scheme 2, beginning with the synthesis of dimeric $[(\text{bme-daco})\text{Fe}]_2$.³¹ The reaction of $[(\text{bme-daco})\text{Fe}]_2$ with either NO^+PF_6^- or $\text{NO}(\text{g})$ in warm MeOH (60 °C) results in a color change from red-brown to green and, ultimately, precipitation of a green solid. The single $\nu(\text{NO})$ stretch at 1649 cm^{-1} is similar to that observed by Baltusis et al., for a related open chain $(\text{N}_2\text{S}_2)\text{Fe}(\text{NO})$ complex.³⁷ The purified complex **2** is thermally and air stable as a solid. As a precaution, solutions were prepared and maintained air free. Air sensitivity, however, is not great even in solution.

Although $[(\text{bme-daco})\text{Fe}]_2$ is largely insoluble in CH_2Cl_2 and CH_3CN , reaction with NO gas draws the compound into these solvents as green complex **2**, in which case further reaction with

(34) Sheldrick, G. *SHELXS-86*: Program for Crystal Structure Solution; Institut für Anorganische Chemie, Universität Göttingen: Göttingen, Germany, 1986.

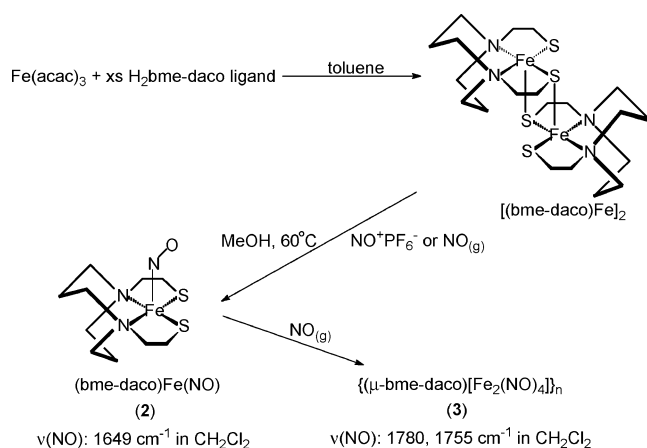
(35) Sheldrick, G. *SHELXL-97*: Program for Crystal Structure Solution; Institut für Anorganische Chemie, Universität Göttingen: Göttingen, Germany, 1997.

(36) *SHELXTL*, version 5.1 or later; Bruker: Madison, WI, 1998.

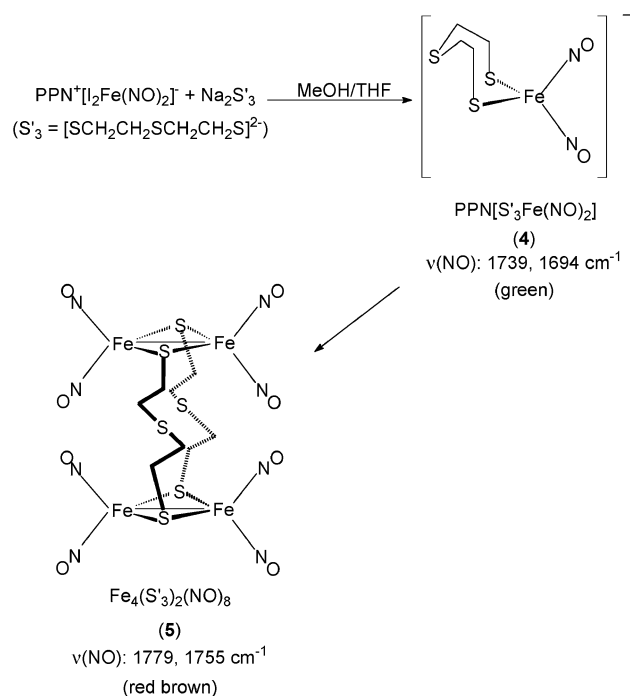
(37) Baltusis, L. M.; Karlin, K. D.; Rabinowitz, H. N.; Dewan, J. C.; Lippard, S. J. *Inorg. Chem.* **1980**, *19*, 2627–2632.

(32) *Smart 1000 CCD*; Bruker Analytical X-ray Systems: Madison, WI, 1999.
(33) *Saint-Plus*, version 6.02; Bruker: Madison, WI, 1999.

Scheme 2



Scheme 3



excess NO readily (within minutes) occurs yielding red-brown derivatives with $\nu(\text{NO})$ absorptions of 1780, 1755 cm^{-1} . In MeOH, complex **2** is more stable toward excess NO, requiring reaction times of ~ 4 h to produce the same red-brown species.

The $\nu(\text{NO})$ bands in the 1750–1780 cm^{-1} region are characteristic of Roussin's red "ester", $(\mu\text{-SR})_2[\text{Fe}(\text{NO})_2]_2$,^{23,38} they are assigned to complex **3** in Scheme 2. Infrared absorptions in this region were also observed in the ultimate reaction product of $\text{I}_2\text{Fe}(\text{NO})_2^-$ with the 2-mercaptoethyl sulfide ligand, S'_3 . Reaction of the sodium salt of $^-\text{SCH}_2\text{CH}_2\text{SCH}_2\text{CH}_2\text{S}^-$ initially produced a green product assigned to the dinitrosyl complex indicated in Scheme 3. All attempts to grow crystals of this presumed monomeric species either at -20 or at 22 °C resulted in a transformation to the red-brown tetranuclear, Roussin's red type species as shown in Scheme 3.

Molecular Structures from X-ray Crystallography. Crystals of complexes **1**, **2**, and **5** were obtained as described in the Experimental Section. Crystallographic data for the structures are given in Table 1. As expected from solubility characteristics, the molecular structure of complex **1** shows no counteranion, which implies a protonated ligand, represented as nitrogen protonation, in Figure 1. Two views of the $(\text{H}^+\text{bme-daco})\text{Fe}(\text{NO})_2$ species are given in Figure 1a and 1b. All atoms of the $\text{Fe}(\text{NO})_2$ unit lie in a plane which bisects that of the FeS_2 portion of the complex; the $\angle\text{N-Fe-N}$ of $115.3(3)^\circ$ and the $\angle\text{S-Fe-S}$ of $111.9(1)^\circ$ are consistent with the nearly regular tetrahedral coordination environment about Fe. The Fe-N-O angles of 168.9° and 166.9° with $\angle\text{O-Fe-O} = 105.5^\circ$ are hallmarks of the so-called "attracto" conformation in which O atoms are drawn in toward each other within the $\text{Fe}(\text{NO})_2$ plane.³⁹ Iron-sulfur and Fe-N bond distances are given in Table 2 and compare well with the $(\text{PhS})_2\text{Fe}(\text{NO})_2^-$ species whose structure was determined as its Et_4N^+ salt.²² Differences of note are largely in the S-C distances, which are ca. 0.07 Å shorter in the $(\text{PhS})_2\text{Fe}(\text{NO})_2^-$ complex.²²

The orientation of complex **1** shown in Figure 1b emphasizes the conformation of the diazacyclooctane ring which, when N-bonded to metals (as seen in complex **2**), forms classic six-membered metal-diazacyclohexane rings resulting in chair-boat conformations. Figure 1b shows the same conformation is maintained in the absence of a transition metal bound to the two nitrogens. The final density map finds a single proton bound to one nitrogen, N(4). This single protonation site was corroborated by the different N-C distances in the N(4) ammonium ion versus the neutral N(3) amine. The geometries of the nitrogens are largely the same according to the $\angle\text{C-N-C}$ angles surrounding N(3) and N(4). The conformation of the ethylene sulfide arms that orient sulfurs to accommodate tetrahedral binding to iron is the first of this type observed for the bme-daco ligand. Typically, the N_2S_2 donor sites of bme-daco support square-planar and square-pyramidal binding.^{31,40} A similar observation has been made for the open chain N_2S_2 ligand, N,N' -dimethyl- N,N' -bis(2-mercaptoethyl)1,3-propanediamine, in the iron-dinitrosyl complex, $(\text{H}^+\text{bme-pda})\text{Fe}(\text{NO})_2$, whose structure was determined on a mixture which was cocrystallized with $(\text{bme-pda})\text{Fe}(\text{NO})_2$.³⁷ The Fe-S and Fe-N distances as well as the coordination angles of the open chain $(\text{H}^+\text{N}_2\text{S}_2)\text{Fe}(\text{NO})_2$ and the more constrained complex **1** are approximately the same, despite the more rigid framework of complex **1**. Overlays of the structures of the open chain and the reinforced diazacycle forms of $(\text{H}^+\text{N}_2\text{S}_2)\text{Fe}(\text{NO})_2$ complexes, and a comparison of the metric data, are given in the Supporting Information.

The molecular structure of complex **2**, $(\text{bme-daco})\text{Fe}(\text{NO})$, given in Figure 2 is that of a square pyramid with an N_2S_2 base and an apical NO group. The iron nitrosyl is substantially bent, $\angle\text{Fe-N-O} = 151.7(5)^\circ$, and the NO vector is oriented in the direction of the basal sulfur atoms. The diazacyclooctane ring adopts its common chair/boat conformations of the fused metallodiazacyclohexane rings, and the ethylene sulfide arms are eclipsed with respect to the $\text{N}_2\text{S}_2\text{Fe}$ coordination group. While the average deviations of N and S atoms from a best planes calculation for the N_2S_2 group are <0.1 Å, the iron atom

(38) (a) Thomas, J. T.; Robertson, J. H.; Cox, E. G. *Acta Crystallogr.* **1958**, *11*, 599–604. (b) Glidewell, C.; Lambert, R. J. *J. Chem. Soc., Dalton Trans.* **1989**, 2061–2064. (c) Glidewell, C.; Harman, M. E.; Bursthouse, M. B.; Johnson, I. L.; Motevalli, M. *J. Chem. Res., Synop.* **1988**, 212–213, 1676–1690. (d) Cai, J.; Mao, S. *Jieyou Huaxue* **1983**, *2*, 263–267.

(39) Martin, R. L.; Taylor, D. *Inorg. Chem.* **1976**, *15*, 2970–2976.

(40) Musie, G.; Lai, C.-H.; Reibenspies, J. H.; Sumner, L. W.; Darensbourg, M. Y. *Inorg. Chem.* **1998**, *37*, 4086–4093.

Table 1. Crystallographic Data for the Fe(NO)/Fe(NO)₂ Complexes

	(H ⁺ bme-daco)Fe(NO) ₂ ^a	(bme-daco)Fe(NO) ^b	Fe ₄ (S ₃) ₂ (NO) ₈ ^b
formula	C ₁₀ H ₂₁ N ₄ O ₂ S ₂ Fe	C ₁₀ H ₂₀ FeN ₃ OS ₂	C ₈ H ₁₆ Fe ₄ N ₈ O ₈ S ₆
fw (g/mol)	349.28	318.26	768.05
crystal system	orthorhombic	monoclinic	triclinic
space group	<i>Pbca</i>	<i>P2₁/n</i>	<i>P1</i>
unit cell			
<i>a</i> (Å)	16.448(10)	7.665(6)	7.7217(8)
<i>b</i> (Å)	12.384(8)	23.861(18)	11.3593(11)
<i>c</i> (Å)	28.996(17)	7.803(6)	15.5075(15)
α (deg)	90	90	98.959(2)
β (deg)	90	112.869(14)	97.956(2)
γ (deg)	90	90	104.367(2)
volume (Å ³)	5906(6)	1315.0(18)	1279.1(2)
<i>Z</i>	16	4	2
<i>R</i> ₁ , ^c <i>wR</i> ₂ ^d (%) [<i>I</i> > 2 σ (<i>I</i>)]	5.81, 12.19	6.40, 14.76	4.43, 11.79
<i>R</i> ₁ , ^c <i>wR</i> ₂ ^d (%) all data	15.46, 14.81	9.01, 16.61	4.84, 12.24

^a Obtained using graphite-monochromatized Mo K α radiation ($\lambda = 0.71073$ Å) at 293 K. ^b Obtained using graphite-monochromatized Mo K α radiation ($\lambda = 0.71073$ Å) at 110 K. ^c $R_1 = \sum ||F_o| - |F_c|| / \sum F_o$. ^d $wR_2 = [\sum [w(F_o^2 - F_c^2)^2] / \sum w(F_o^2)^2]^{1/2}$.

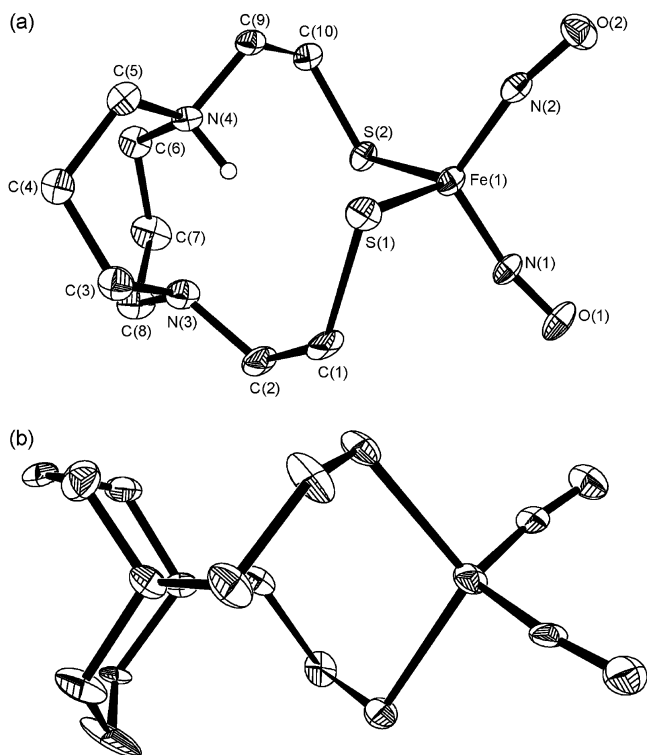


Figure 1. Two views of the molecular structure of complex **1**, (H⁺bme-daco)Fe(NO)₂, with thermal ellipsoids drawn at the 50% probability level. Selected distances and angles are given in Table 2.

is displaced by 0.476 Å out of the plane and toward the apical NO. This is similar to the open chain analogues, (bme-pda)-Fe(NO) and *N,N'*-dimethyl-*N,N'*-bis(2-mercaptoethyl)ethylenediamine iron nitrosyl or (bme-eda)Fe(NO), in which the Fe is displaced by 0.55 and 0.415 Å, respectively, from the N₂S₂ basal planes.^{37,41} Interestingly, the displacement of Fe from the N₂S₂ plane toward the apical S in the dimeric [(bme-daco)Fe]₂ complex which is the precursor to the (bme-daco)Fe(NO) is even greater, 0.59 Å.⁴⁰ The iron to nitrogen distance of Fe–NO is 1.707(6) Å in complex **2**; this is 0.3 Å less than the Fe–N distances to the N₂S₂ ligand.

The tetranuclear complex **5** consists of a dimer of (μ -SR)₂[Fe(NO)₂]₂ units in which the μ -SR is a dithiolate, [−]SCH₂CH₂–

Table 2. Selected Distances and Angles of Complexes **1**, (H⁺bme-daco)Fe(NO)₂, and **5**, Fe₄(S₃)₂(NO)₈ (See Figures 1 and 3)

	1	5
Fe–N ₁ (Å)	1.657(6)	1.669(2)
Fe–N ₂	1.681(6)	1.681(3)
Fe–S ₁	2.270(2)	2.255(1)
Fe–S ₂	2.285(3)	2.249(1)
N ₁ –O ₁	1.196(7)	1.172(3)
N ₂ –O ₂	1.175(7)	1.164(3)
S ₁ –C ₁	1.837(7)	1.837(3)
S ₂ –C ₁₀	1.824(7)	1.830(3)
Fe–Fe _{avg}		2.677(6)
Fe–Fe		6.861(1)
S–S	3.769(1)	3.618(1)
Fe–N(R ₂) _{avg}	4.113(1)	
\angle N ₁ –Fe–N ₂ (deg)	115.3(3)	119.1(1)
\angle N–Fe–S _{avg}	107.6(2)	107.3(9)
\angle Fe–N–O _{avg}	167.9(6)	171.5(2)
\angle S ₁ –Fe–S ₂	111.8(1)	107.0(3)
\angle Fe–S–Fe		72.9(3)
\angle Fe–S–C _{avg}	108.3(3)	108.0(1)

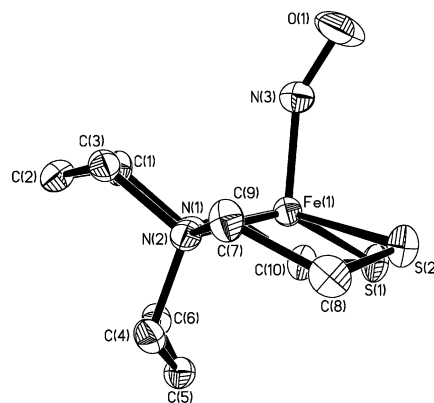


Figure 2. Molecular structure of complex **2**, (bme-daco)Fe(NO), with thermal ellipsoids drawn at the 50% probability level. Selected distances, Å: Fe–N₁, 2.069(5); Fe–N₂, 2.072(5); Fe–N₃, 1.707(6); Fe–S₁, 2.239(2); Fe–S₂, 2.253(2); N₃–O₁, 1.165(6); S–N_{avg}, 1.824(6). Selected angles, deg: \angle N₁–Fe–N₂, 87.0(2); \angle N₁–Fe–N₃, 87.0(2); \angle N₁–Fe–S₁, 87.8(2); \angle N₁–Fe–S₂, 149.4(1); \angle Fe–N–O, 151.7(5); \angle S₁–Fe–S₂, 88.11(8).

SCH₂CH₂S[−], and serves to link individual Fe₂(NO)₄ units, Figure 3a. The alternate view of the molecular structure in Figure 3b emphasizes that all 4 iron, 8 nitrogen, and 8 oxygen atoms are in the same plane. The planar 2Fe₂S core of the (μ -SR)₂[Fe(NO)₂]₂ units is diamond-shaped with \angle S–Fe–S of 107.0° and \angle Fe–S–Fe of 72.9°; the Fe–Fe distance averages to 2.68

(41) Karlin, K. D.; Rabinowitz, H. N.; Lewis, D. L.; Lippard, S. J. *Inorg. Chem.* **1977**, *16*, 3262–3267.

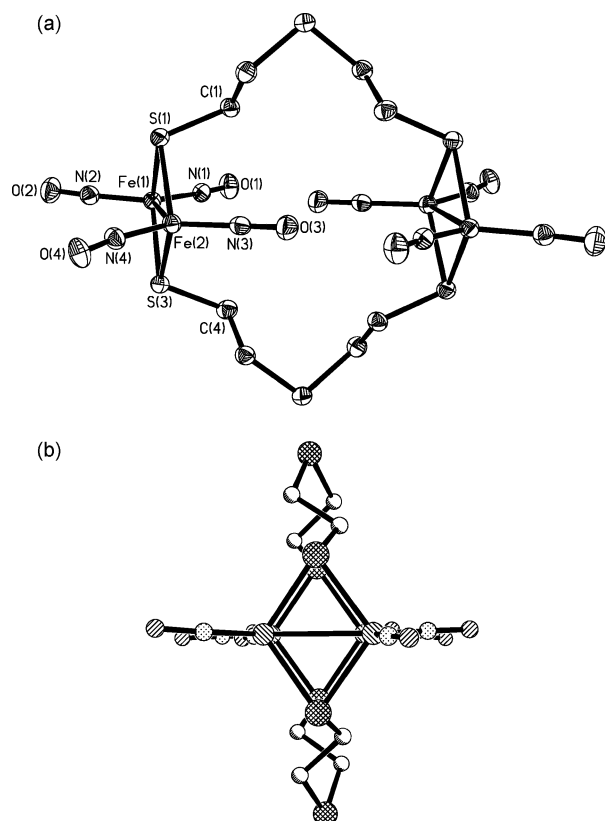
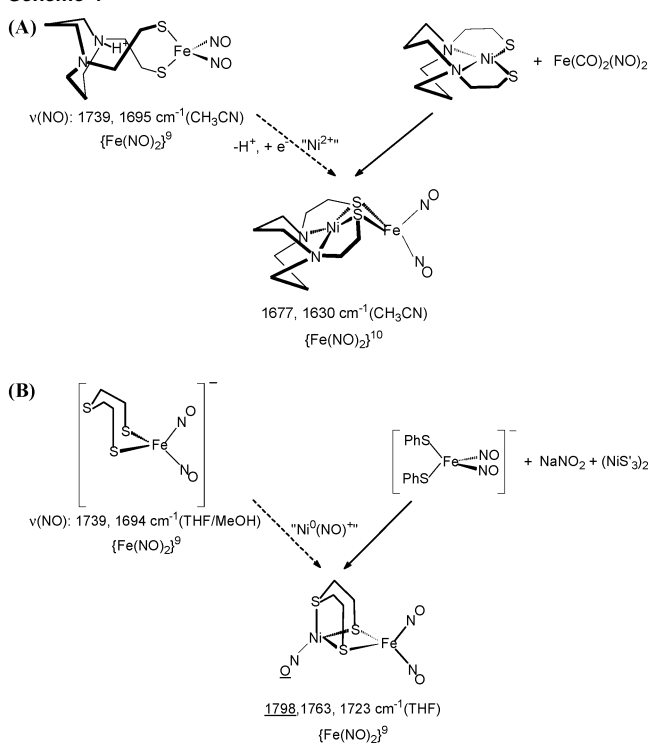


Figure 3. (a) Molecular structure of complex **5**, $\text{Fe}_4(\text{S}'_3)_2(\text{NO})_8$, with thermal ellipsoids drawn at the 50% probability level. Selected distances and angles are given in Table 2. (b) Alternate view, perpendicular to the Fe–Fe bond vector, using the ball-and-stick representation.

Å. The $2\text{Fe}2\text{S}$ plane of each $(\mu\text{-SR})_2[\text{Fe}(\text{NO})_2]_2$ unit bisects the $\text{Fe}(\text{NO})_2$ planes, yielding pseudo-tetrahedral coordination geometry about each iron. The $\angle\text{N-Fe-N}$ of 119.1° is 4° greater than that of the $\text{Fe}(\text{NO})_2$ unit of complex **1**. The $2\text{Fe}2\text{S}$ planes of individual $(\mu\text{-SR})_2[\text{Fe}(\text{NO})_2]_2$ units are parallel and eclipsed with Fe...Fe spacings across the 16-membered ring of 6.86 Å. Complex **5** is a dimeric form of Roussin's red ester, $(\mu\text{-SR})_2[\text{Fe}_2(\text{NO})_4]$, known to exist in solution as a mixture in C_{2h} and C_{2v} isomer forms.⁴² While the known crystal structures of dimeric Roussin's red esters are of the C_{2h} isomeric forms with $\mu\text{-RS}$ groups in the anti-conformation,⁴³ the linking of individual units in complex **5** by $\mu\text{-SCH}_2\text{CH}_2\text{SCH}_2\text{CH}_2\text{S-}\mu$ dithiolate restricts the geometry to the syn orientation of all $\mu\text{-S-C}$ bonds.

Spectral Characterizations: $\nu(\text{NO})$ Infrared Data. The $\nu(\text{NO})$ IR values for the new complexes are listed in the schemes. Literature precedents for the oxidized monomeric $\{\text{Fe}(\text{NO})_2\}^9$ units may be found in the anionic halide series $\text{X}_2\text{Fe}(\text{NO})_2^-$ which vary little with X^- in CH_2Cl_2 solutions ($\text{X} = \text{Cl}$, 1781, 1708 cm^{-1} ; Br, 1780, 1710 cm^{-1} ; I, 1778, 1719 cm^{-1}).²¹ Reported $\nu(\text{NO})$ IR data for thiolate derivatives are, to our knowledge, very limited. We find the $\nu(\text{NO})$ values for the CH_2Cl_2 solution spectrum of the $(\text{PhS})_2\text{Fe}(\text{NO})_2^-$ derivative as its PPN^+ salt are at 1745 and 1697 cm^{-1} (1737 and 1693 cm^{-1} in THF). These values compare well to the two alkanethiolates of our study, $(\text{H}^+\text{bme-daco})\text{Fe}(\text{NO})_2$, complex **1**, with $\nu(\text{NO}) = 1739$ and 1695 cm^{-1} (THF); 1746, 1698 cm^{-1} ($\text{CH}_2\text{-}$

Scheme 4



Cl_2), and the $\text{S}_3\text{Fe}(\text{NO})_2^-$, complex **4**, where $\nu(\text{NO}) = 1739$ and 1694 cm^{-1} in THF/MeOH. The shifts of $\nu(\text{NO})$ to lower wavenumbers in the aryl and alkanethiolates as compared to the halides are consistent with the better donor character, specifically the better π -donor ability, of the thiolate sulfurs as compared to that of the halides.

Shown in Scheme 4 are the $\nu(\text{NO})$ spectral changes which occur on attaching nickel to the thiolate sulfurs which bind the $\text{Fe}(\text{NO})_2$ units in monomeric $(\text{SRS})\text{Fe}(\text{NO})_2^-$. The dashed line arrows in Scheme 4A represent Gedanken (thought) experiments only as the known syntheses of the NiFe complexes are via the alternate routes represented by the solid line arrows. That is, we have not been able to displace the proton in complex **1** by insertion of a Ni^{2+} into the N_2S_2 binding site. In fact, as noted, the IR spectral data imply the $\text{Fe}(\text{NO})_2$ units are in different oxidation levels in the nickel-free versus the nickel-bound forms of $(\text{bme-daco})\text{Fe}(\text{NO})_2$.²⁸ The former is analogous to that of the X^- and PhS^- derivatives which stabilize the oxidized form or $\{\text{Fe}(\text{NO})_2\}^9$, while the latter supports the reduced $\{\text{Fe}(\text{NO})_2\}^{10}$ form. Thus, the formal displacement of a proton by Ni^{2+} would have to be accompanied by a conformational change of the N_2S_2 ligand as well as addition of an electron which serves to reduce the $\{\text{Fe}(\text{NO})_2\}^9$ to $\{\text{Fe}(\text{NO})_2\}^{10}$. The latter conclusion is supported both by the lower $\nu(\text{NO})$ stretching frequencies as well as by the similarity of the IR data to diphosphine derivatives of $\{\text{Fe}(\text{NO})_2\}^{10}$.

Equation B of Scheme 4 shows that the $\nu(\text{NO})$ spectral changes on binding the nickel-zero containing fragment $\text{Ni}(\text{NO})^+$ to the metal-free $\text{S}_3\text{Fe}(\text{NO})_2^-$ result in shifts to higher energies, implying the electron density available from the thiolate donors has been diminished by interaction with the $\text{Ni}(\text{NO})^+$ moiety. The values for the Ni^0 -metalated dithio-DNIC are relatively close to those for the iodide complex, $\text{I}_2\text{Fe}(\text{NO})_2^-$, vide supra, which also contains the oxidized version of $\{\text{Fe}(\text{NO})_2\}^9$.

(42) Butler, A. R.; Glidewell, C.; Johnson, I. L. *Polyhedron* **1987**, *6*, 1147–1148.

(43) Butler, A. R.; Glidewell, C.; Hyde, A. R.; Walton, J. C. *Polyhedron* **1985**, *4*, 797–809.

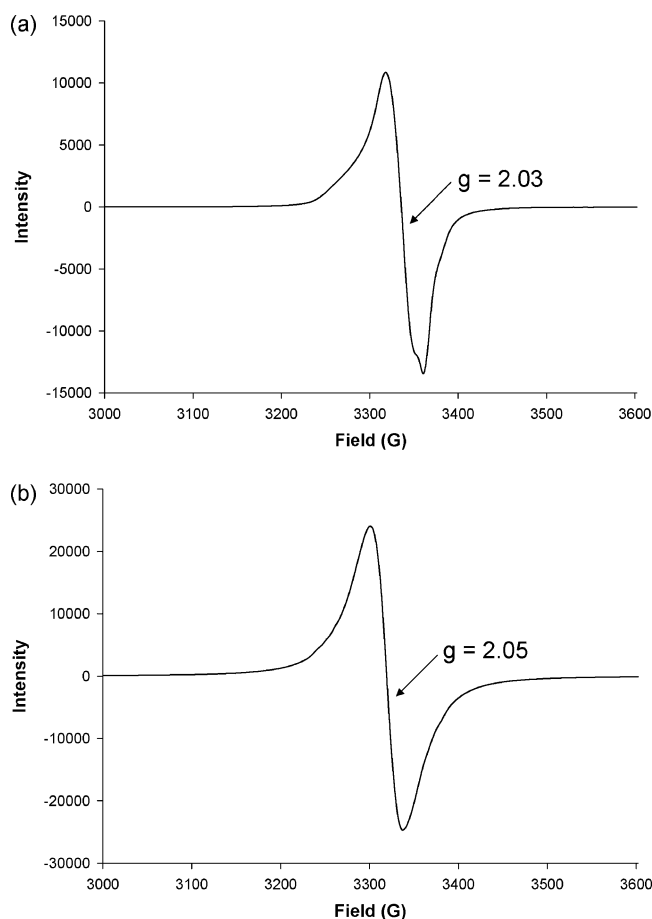


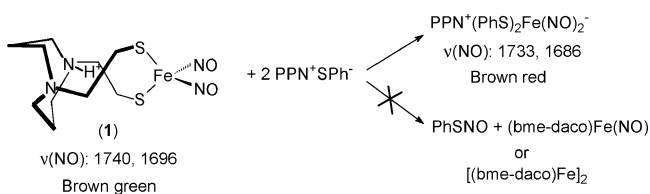
Figure 4. (a) EPR spectrum of complex **1** in CH_2Cl_2 at 10 K; (b) of complex **2** in CH_2Cl_2 at 77 K.

Magnetism and EPR Data. Complexes **1** and **2** are paramagnetic and show a single isotropic signal in their EPR spectra with g -values of 2.03 and 2.05, respectively, Figure 4. The former value is typical of dinitrosyl iron complexes in which the $\text{Fe}(\text{NO})_2$ unit is in the oxidized form, that is, $\{\text{Fe}(\text{NO})_2\}^9$.²³ The latter has precedent in the open chain, mononitrosyl complex, that is, the $\text{N}_2\text{S}_2\text{Fe}(\text{NO})$ complexes reported by Lippard et al., which implicates an electronic configuration of $\{\text{Fe}(\text{NO})\}^7$.⁴¹ While the Roussin's red ester dimer, complex **5**, as well as the presumed $(\mu\text{-bme-daco})_2[\text{Fe}_2(\text{NO})_4]$ should be diamagnetic, complicated EPR signals are observed. These are assumed to arise from paramagnetic species formed from various solvent interactions.

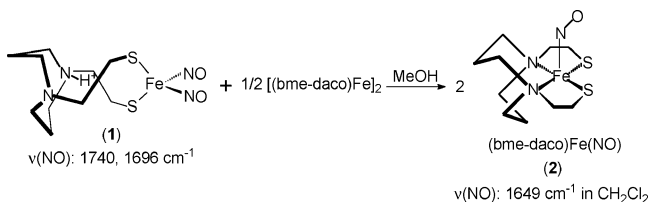
Chemical Reactivity. As background for establishing reaction patterns which might relate to the biological significance of iron dinitrosyl complexes, we have explored the reactivity of $(\text{H}^+\text{-bme-daco})\text{Fe}(\text{NO})_2$, as a model for a protein-bound DNIC, with a thiolate and a thiol, PhS^- and PhSH , respectively. Two major reaction paths were anticipated for PhS^- . (1) PhS^- might displace the $^-\text{SRS}^-$ dicysteine mimic, generating the known and presumably more stable $(\text{PhS})_2\text{Fe}(\text{NO})_2^-$. (2) Alternatively, PhS^- might remove NO from iron in a nucleophilic attack process, generating PhSNO , with the remaining FeNO shifting into the N_2S_2 binding site. With removal of both NO's, the $[(\text{bme-daco})\text{Fe}]_2$ might be reclaimed.

Scheme 5 presents the results of IR and UV/vis monitors of the reaction of complex **1** with PPN^+SPh^- . Note that the $\nu(\text{NO})$ values of the reactant **1** and the expected product $(\text{PhS})_2\text{Fe}(\text{NO})_2^-$

Scheme 5



Scheme 6



are extremely close in solution, necessitating extensive control experiments for credible interpretation. In comparative studies, THF solution samples of (a) pure complex **1**, (b) complex **1** plus PPN^+SPh^- , and (c) pure $\text{PPN}^+[(\text{PhS})_2\text{Fe}(\text{NO})_2]^-$ were prepared at 0°C , and their $\nu(\text{NO})$ IR spectra and UV/vis spectra were recorded. The pure sample of complex **1**, over the extended time-course of this experiment, showed only a slight decomposition (ca. 5%) to the Roussin's red derivative $[(\text{bme-daco})\text{Fe}(\text{NO})_2]_n$. Immediately on addition of 2 equiv of PPN^+SPh^- (in $\text{THF}/\text{CH}_3\text{CN} = 10/1$ mixture) to complex **1**, the solution color changed from the brown-green to the brown-red characteristic of the $\text{PPN}^+[(\text{PhS})_2\text{Fe}(\text{NO})_2]^-$ sample. The $\nu(\text{NO})$ bands shifted from those observed for the pure complex **1** to the more negative values of $\text{PPN}^+[(\text{PhS})_2\text{Fe}(\text{NO})_2]^-$. After 3 h at 0°C and on warming to 25°C and holding for 10 h, the color did not change and the IR spectrum indicated $[(\text{PhS})_2\text{Fe}(\text{NO})_2]^-$ was the major product. There was no $\nu(\text{NO})$ band at $\sim 1650\text{ cm}^{-1}$, which would have indicated the presence of mono-nitrosyl product. Under similar conditions, no reaction was observed with PhSH in a 10-fold excess.

Thiolate and thiol ligand exchange processes of Roussin's red esters have previously been reported by Glidewell et al.⁴³ Studies of diamagnetic, dimeric $(\mu\text{-SR}')_2\text{Fe}_2(\text{NO})_4$ found solvent dependencies and paramagnetic mononuclear solvated products which implicated highly complex reaction pathways.⁴³

Complex **1** was found to react with $[(\text{bme-daco})\text{Fe}]_2$ in stoichiometric amounts as described in Scheme 6. A mixed-solvent system, $\text{MeOH}/[(\text{bme-daco})\text{Fe}]_2$ and $\text{CH}_2\text{Cl}_2\text{-MeOH}/$ complex **1**, was required for solubilization. On mixing such solutions at 0°C , no change was observed over 1 h. Upon warming the solutions to 22°C and stirring for 4 h, the color changed to green and a single band in the IR spectrum, at 1649 cm^{-1} for the mono-nitrosyl, grew in. The final IR spectrum (after the solution was left overnight at 22°C) showed only complex **2**. It should be noted that complex **1** is stable in solution over the same time period, decomposing over a longer time to the Roussin's red ester described above.

Summary and Comments

The chelating dithiolate based on the structurally reinforced bme-daco has been demonstrated to serve as a bidentate ligand to the tetrahedral iron of the $\text{Fe}(\text{NO})_2$ unit, forming overall a 12-membered ring system. In a different conformation, the ligand captures $\text{Fe}(\text{NO})$ within its N_2S_2 core to yield a square

pyramid with apical NO. Excess NO readily leads to the thermodynamically stable Roussin's red esters, typically formulated as $(\mu\text{-SR})_2\text{Fe}_2(\text{NO})_4$. While the $[(\text{bme-daco})\text{Fe}_2(\text{NO})_4]_n$ complex could not be crystallized, its distinctive $\nu(\text{NO})$ bands are similar to those of the $(\mu\text{-SCH}_2\text{CH}_2\text{SCH}_2\text{CH}_2\text{S})_2[\text{Fe}_2(\text{NO})_4]_2$, complex **5**.

Our work establishes that the major chemical components of iron nitrosyl complexes involving N_2S_2 coordination sites may be distinguished by $\nu(\text{NO})$ IR spectroscopy. This result was useful in preliminary studies of thiolate ligand exchange and NO transfer from Fe. To our knowledge and as of this writing, the controversy regarding iron dinitrosyls as possible NO carriers in vivo, versus their being irrevocably protein bound, has not been resolved. Our results indicate that the $\text{Fe}(\text{NO})_2$ is indeed transferable as a unit to a different thiolate ligand as implicated in the biological studies of Vanin et al.⁴⁴ As the role of NO in physiology continues to expand, such spectroscopic and reaction model studies as those above are a

vital requirement for deciphering and predicting potential reaction pathways.

Acknowledgment. We acknowledge the financial support of the National Science Foundation (grants CHE 01-11629 to M.Y.D. for this work, CHE 00-92010 for the EPR instrument, and CHE 98-07975 for the purchase of X-ray equipment) and contributions from the Robert A. Welch Foundation. We appreciate the assistance of Dr. J. C. Yarbrough, M. V. Rampersad, and Dr. D. Chong. Collaborations with Dr. W.-F. Liaw, National Tsing Hua University, Taiwan, initiated this project.

Supporting Information Available: Tables of crystal data and experimental conditions for the X-ray studies, atomic coordinates, and B_{eq} values, complete listings of bond lengths and bond angles, and anisotropic temperature factors for complexes **1**, **2**, and **5** (PDF, CIF). This material is available free of charge via the Internet at <http://pubs.acs.org>.

JA049627Y

(44) Mülsch, A.; Mordvintcev, P.; Vanin, A. F.; Busse, R. *FEBS Lett.* **1991**, *294*, 252–256.